

Chapter 10

Air Flow Entrainment of Lactose Powder: Simulation and Experiment



Thomas Kopsch, Darragh Murnane and Digby Symons 

Abstract Lactose powder is frequently used as an excipient in drug formulations for use in dry powder inhalers (DPIs). As a patient inhales through a DPI the lactose powder is entrained into the airflow, thus enabling delivery of the drug dose to the patient's lungs. Computational fluid dynamics (CFD) can potentially aid the designers of DPIs if the entrainment process can be accurately simulated. In this study we compare CFD simulations and experimental observations of entrainment of lactose powder using an example 2D DPI geometry and typical inhalation airflow profiles. 2D transient CFD simulations were carried out using an Eulerian-Eulerian solver to model the progression of entrainment subject to two example patient inhalation maneuvers: one high and one low flow rate. Experiments used the same 2D geometry laser cut from a 3 mm thick opaque acrylic sheet sandwiched between transparent sheets. A powder dose was pre-loaded before assembly of the geometry. Two different lactose powders were used with particle sizes of 59 and 119 μm . Air flow was provided by a computer controlled pump (a breath simulator). The geometry was back lit and the progression of entrainment was filmed at 1000 fps. Comparison of the CFD simulations and experimental results showed good agreement for the two powders tested.

Keywords Multiphase flow · CFD · Validation

T. Kopsch
Engineering Department, University of Cambridge, Cambridge, UK

D. Murnane
Department of Pharmacy, University of Hertfordshire, Hatfield, UK

D. Symons (✉)
Mechanical Engineering Department, University of Canterbury, Christchurch, New Zealand
e-mail: digby.symons@canterbury.ac.nz

© Springer Nature Switzerland AG 2019
S. Gutschmidt et al. (eds.), *IUTAM Symposium on Recent Advances in Moving Boundary Problems in Mechanics*, IUTAM Bookseries 34,
https://doi.org/10.1007/978-3-030-13720-5_10

10.1 Introduction

10.1.1 Motivation

Dry powder inhalers (DPIs) are used to deliver medicines directly to the lungs to treat both respiratory and systemic diseases. Drug particles are usually micronized to obtain particle sizes of less than $5\ \mu\text{m}$ to maximize pulmonary deposition and minimize tracheobronchial deposition [1]. However, such small particles are typically extremely cohesive: they have poor flowability and form large agglomerates that are difficult to entrain into the airstream. The drug is therefore often pre-mixed with an excipient composed of larger carrier particles. De-agglomeration of the drug from the carrier particles is accomplished (primarily by impacts) as the entrained formulation exits the DPI.

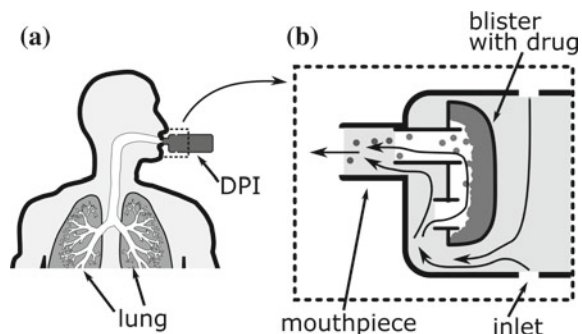
Lactose powder is frequently used as an excipient in drug formulations for use in dry powder inhalers (DPIs). In many DPIs the powder drug dose is stored in a foil sealed “blister” until use. Typically the foil seal is then pierced by an inlet and outlet tube and the blister itself forms the entrainment part of the air path through the DPI, see Fig. 10.1.

Good performance of the entrainment geometry of a DPI is necessary to achieve good drug delivery performance. Computational fluid dynamics (CFD) can potentially aid the designers of DPIs if the entrainment process can be accurately simulated.

10.1.2 Overview of Paper

In this study we compare CFD simulations and some initial experimental observations of entrainment of lactose powder using an example DPI geometry and typical patient inhalation airflow profiles.

Fig. 10.1 Schematic illustration of the drug delivery process with a DPI. **a** The DPI and the respiratory tract. **b** A close-up view of the DPI



10.2 Methods

10.2.1 Computational Simulation

For this study the example entrainment geometry investigated was a 2D representation of a blister type entrainment geometry with length ~ 6 mm, see Fig. 10.2 The geometry had previously been computationally optimised to perform consistently, with low sensitivity to the patient's inhalation profile, using a similar process to that described in Kopsch et al. [2].

In CFD analysis for DPIs the particulate (drug) phase can either be ignored (a single phase approach considering air flow only) or modelled using a multiphase approach. The majority of reported studies using multiphase approaches for simulation of DPIs have used Eulerian-Lagrangian (EL), i.e. particle-tracking, approaches [3]. However, EL approaches make it difficult to study the fluidization process of a powder bed due to the large number of particle-particle interactions. It is for this reason that Zimarev et al. [4] introduced an Eulerian-Eulerian (EE) CFD approach to model the entrainment of drug in a DPI and to optimize the entrainment part of a DPI. When the volume fraction of drug is very high, the EE approach is more computationally efficient than an EL particle tracking approach.

In the EE approach, the drug particles are modelled as a second continuous phase and the interaction between the gas and the granular phase is modelled. A new

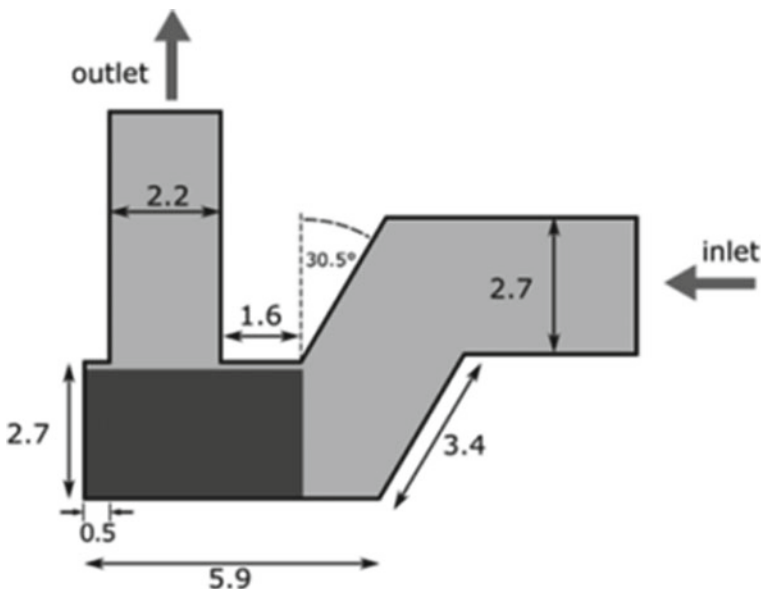


Fig. 10.2 The tested geometry with dimensions in mm indicated. The dark grey area indicates the initial powder load in the CFD simulations

Fig. 10.3 Idealized representation of the Eulerian-Eulerian (EE) approach. The volume fraction α indicates the density of particles

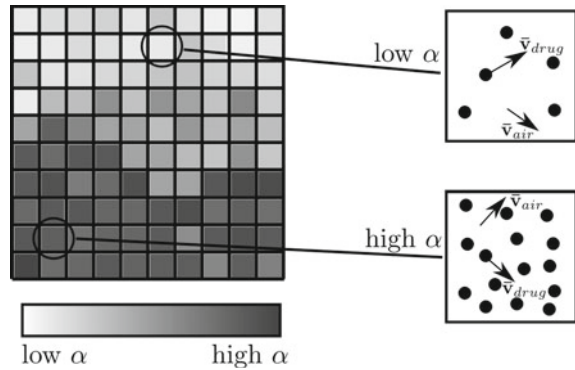


Table 10.1 Settings for the OpenFOAM EE CFD solver

CFD modelling parameter	Sub-model selected
Granular viscosity model	'Gidaspow' [7]
Frictional stress model	'Johnson Jackson' [8]
Conductivity model	'Gidaspow' [7]
Granular pressure model	'Lun' [5, 9]
Radial distribution	'Lun Savage' [5, 9]
Drag coefficient	'GidaspowErgunWenYu' [7]

variable, the volume fraction (α) is introduced to keep track of the local fraction of granular phase. As in other CFD approaches the domain of interest is split into a large number of cells. For each cell the EE algorithm solves for a number of variables including the volume fraction α , the average velocity of drug particles \bar{v}_{drug} and the average velocity of the gaseous phase \bar{v}_{air} . As shown in Fig. 10.3 the value of α indicates the number of particles in that cell. In an EE approach, all phases, including the particulate phases, are modelled as continuous fluids and consequently mass, momentum and energy conservation laws are applied to all phases. In many cases, these equations look similar to the standard Navier-Stokes equations. The kinetic theory of granular flow (KTGF) [5] is one method to model the constitutive behaviour of a granular phase in the EE approach. KTGF makes predictions about stresses and phase interaction terms in the governing equations of the fluid.

For this study 2D transient CFD simulations were carried out using "twoPhaseEulerFoam": an OpenFoam [6] EE solver with $k-\epsilon$ turbulence modelling. KTGF sub-models of particle-particle interaction were used to provide the constitutive behaviour of the powder phase. The sub-models used in this work are given in Table 10.1.

The powder was modelled as uniform sized particles with diameter equal to the measured D50 size of the lactose powders used in the later experiments, i.e. 59 and 119 μm , see Table 10.2. The simulations modelled the progression of entrainment

Table 10.2 Powder characteristics of two different lactose powders

Manufacturer	DMV-Fonterra Excipients GmbH & Co. KG			
Product name	Respitose® SV003		Respitose® Lactohale 100	
	Measured	Specification	Measured	Specification
D10 (μm)	33.1 ± 0.2	19–43	50.9 ± 0.6	45–65
D50 (μm)	59.2 ± 0.1	53–66	119.4 ± 0.4	125–145
D90 (μm)	89.9 ± 0.3	75–106	200.4 ± 2.4	200–250
Poured density (g/L)		630		690
Tapped density (1250 taps) (g/L)		780		840

subject to two time varying flow rate profiles representative of typical patient inhalation maneuvers: one high and one low flow rate.

10.2.2 Experiment

Lactose Powders

Experiments were carried out with two different powders: Respitose SV003 and Lactohale 100 (measured D50 of 59 and 119 μm respectively, both DMV-Fonterra Excipients GmbH). The material properties as specified by the manufacturer are shown in Table 10.2. Most real pharmaceutical powders, including the lactose powders chosen in this study, are not monodisperse in size (as assumed for the CFD simulations). Instead, they consist of particles of a range of different diameters. Table 10.2 shows the D10, D50 and D90 values for these powders as specified by the manufacturer. To validate these specifications a measurement of particle size distribution was carried out. The particle size distribution for was measured with a laser diffraction system, a Sympatec HELOS laser diffraction sensor [10] together with a Sympatec RODOS dry dispersing unit [11]. Measured values are included in Table 10.2 where the stated error is the standard deviation over four repeated measurements. Measured values are generally in agreement with the specification.

Entrainment Module

Entrainment experiments were carried out with an apparatus based on the same 2D geometry as used for the CFD simulations. The geometry was laser cut from a 3.15 mm thick opaque acrylic sheet that was then clamped between two transparent acrylic sheets, see Fig. 10.4. The experimental powder dose was pre-loaded before assembly of the geometry.

Breathing Simulator

In order to simulate a patient's inhalation maneuver, a breathing simulator (model BRS 3000 [12] from Copley Scientific) was used. The breathing simulator could

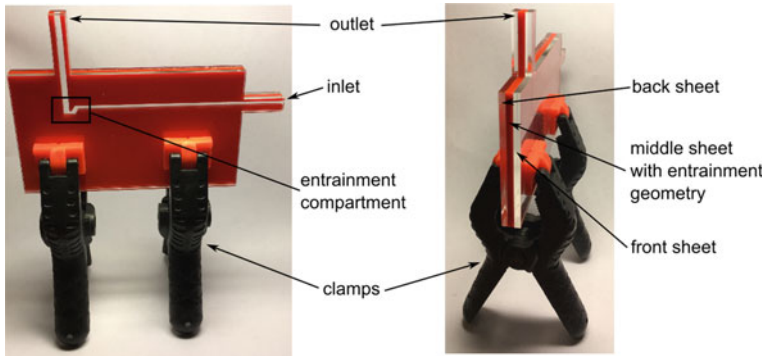


Fig. 10.4 Assembled entrainment module

generate user-defined inhalation flow rate profiles. It consists of a piston whose movement is controlled by a microprocessor. Integrated software allows a flow rate profile to be specified. The breathing simulator was connected to the outlet of the entrainment unit via a filter. The purpose of the filter was to remove powder from the air flow before it entered the breathing simulator. A digital flow meter (Certifier FA Plus Ventilator Test System 4080 [13] by TSI Inc.) was connected to the inlet of the entrainment unit. The flow meter monitored the specified flow rate profile. Figure 10.5 depicts schematically the position of the breathing simulator, the entrainment module and the flow meter.

Camera and Illumination

During the entrainment process, the entrainment compartment was filmed with a high-speed camera. The camera (Casio Exilim EX-FH20 [14]) was set to high-speed mode (1000 frames per second). It was mounted with a tripod screw on a wooden platform to fix the relative position of the camera and the entrainment module. The goal was to obtain the same image section consistently in different experiments. The entrainment module was illuminated from the back. A diffusion panel (a thin sheet of paper) was placed between the lamp and the entrainment module to reduce optical artefacts. Figure 10.6 shows two photos of the complete experimental setup.

Inhalation Flow Rate Profiles

The specified flow rate profiles $Q_{\text{high}}(t)$ and $Q_{\text{low}}(t)$ are shown in Fig. 10.7. Both flow rate profiles started with the inhalation maneuver at time $t = 0$ s. The maximum flow rate of the inhalation profile was reached at time $t = 0.45$ s after the onset of the inhalation. For the ‘high’ flow rate profile the peak flow was 20 L min^{-1} , for the ‘low’ flow rate profile the peak was 14 L min^{-1} . Since an air bypass was not incorporated in the entrainment module, the chosen peak values were lower than typical peak values of real patients [15] to account for the absent bypass. For both profiles, inhalation was complete at time $t = 3.7$ s. At this time, most of the powder

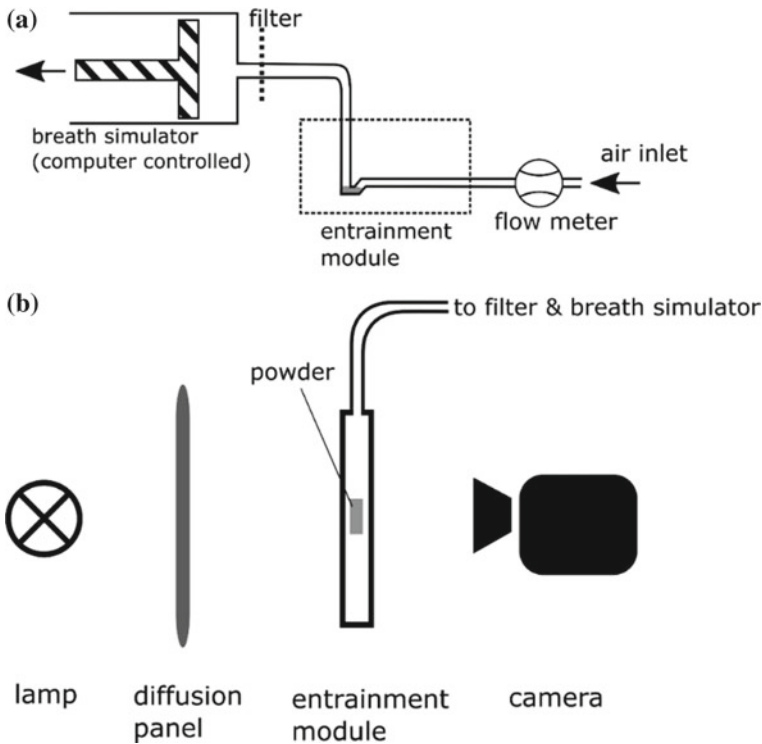


Fig. 10.5 Setup of the entrainment experiment. **a** Front view: the breathing simulator generates a flow through the entrainment module. **b** Side view: a camera records the powder in the entrainment module

was typically entrained. However, video post-processing is simplified if a reference frame with the evacuated entrainment unit is available. Consequently, a high flow rate was applied from time $t = 5$ to 11 s to evacuate the entrainment unit completely. The exact length and strength of the evacuation flow profile was not important as long the compartment was emptied. As an illustration, Fig. 10.7b shows how the distribution of drug in the entrainment compartment may look as a function of time.

Analysis of the Entrainment Videos

The aim of analysing the entrainment videos was to compare the experimental observations of the entrainment process with predictions from CFD simulations. This was done both qualitatively and quantitatively. Qualitatively, individual frames from an entrainment video were compared with the corresponding CFD contour plots of the volume fraction α . Quantitatively, the mass of drug released $M(t)$ as a function of time t was determined from the videos and compared to CFD predictions.

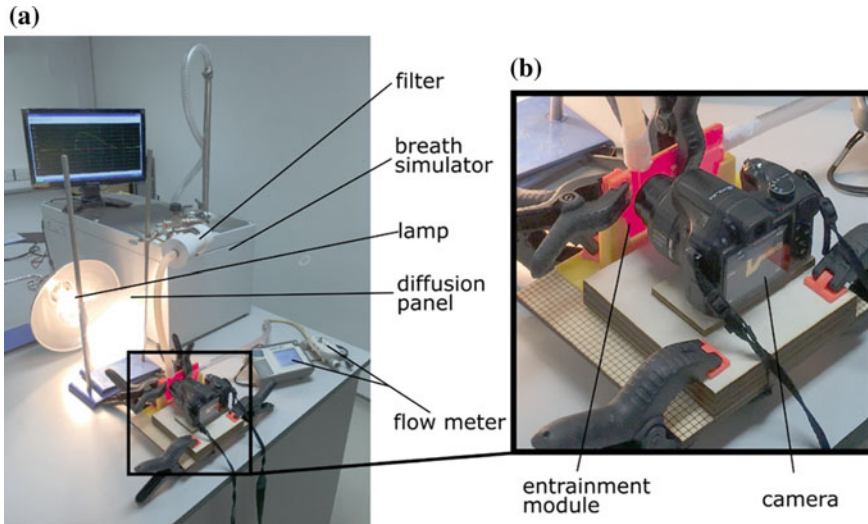


Fig. 10.6 Setup of the entrainment experiment. The breathing simulator generates a flow rate profile through the entrainment module, while a camera records the process

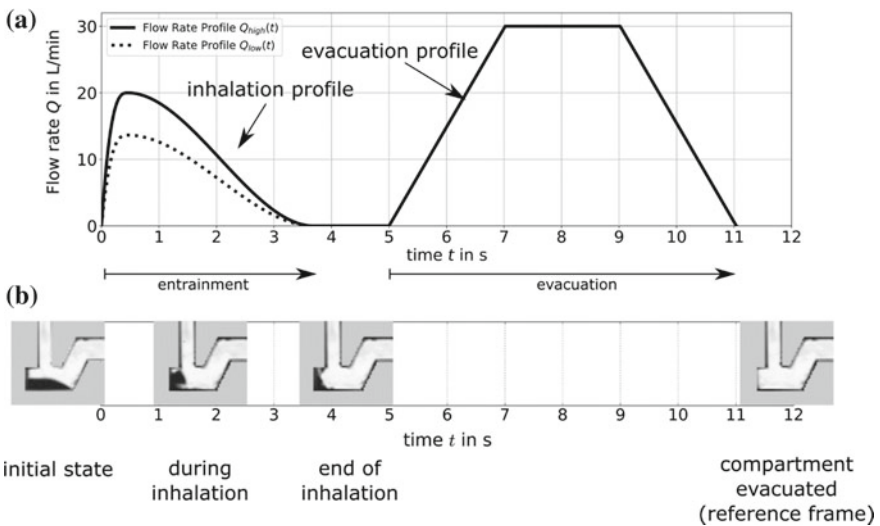


Fig. 10.7 **a** The specified inhalation flow rate profiles $Q_{high}(t)$ and $Q_{low}(t)$. The entrainment time interval and the evacuation time interval are indicated. **b** An illustration of the entrainment process as a function of time (sample data for illustration only)

10.3 Results

For both powders SV003 and LH100 experimental entrainment results were compared to CFD predictions. A qualitative comparison of video frames and CFD contour plots of the volume fraction α for the ‘high’ flow profile are shown in Fig. 10.8. The CFD prediction is in good agreement with the experimental video footage for both powders.

Figure 10.9 compares the predicted mass release profile $M(t)$ and the corresponding experimental measurement for both ‘high’ and ‘low’ flow profiles. Each experimental curve is the average of three experiments. Good agreement between the CFD prediction and the experiment is observed.

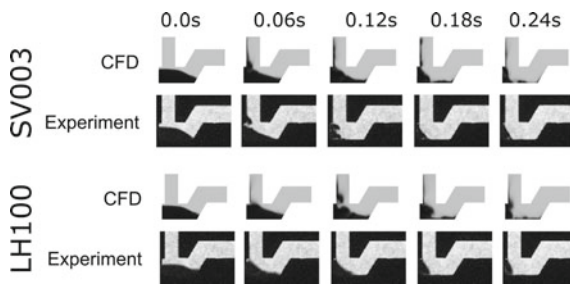


Fig. 10.8 Comparison of CFD and experimental images of entrainment with the high flow profile. Air flow is from right to left

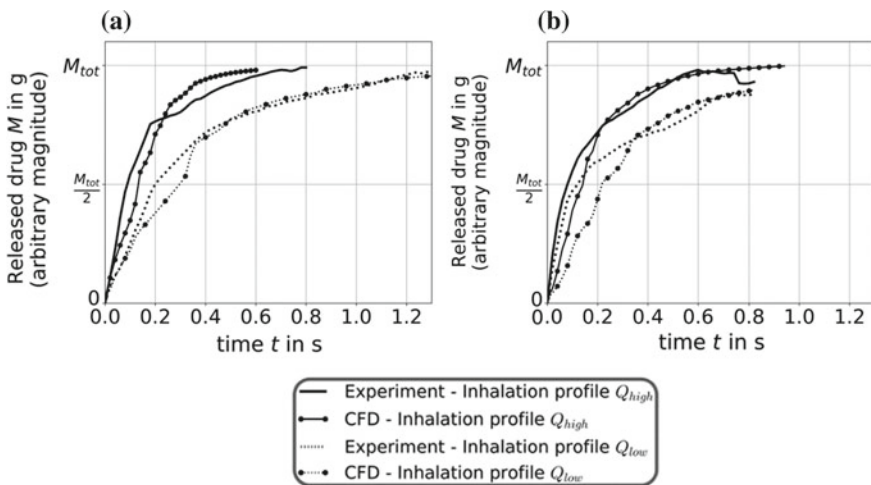


Fig. 10.9 Comparison of predicted (CFD) and experimentally measured drug powder release with both the high and low flow profiles. **a** SV003 **b** LH100

10.4 Conclusions

The aim of this work was to make a preliminary experimental validation of the EE CFD method for simulating entrainment of lactose in an example DPI geometry. This was achieved by conducting entrainment experiments with a transparent entrainment module, two different lactose powders and two different inhalation flow rate profiles. Entrainment processes were recorded with a high-speed camera and the resulting video footage was compared qualitatively and quantitatively with the corresponding CFD prediction. For the quantitative comparison $M(t)$, the mass of released drug, was inferred from the measured intensity distribution.

Limitations of the EE CFD method used were that cohesive interaction and deagglomeration of particles were not modelled. Nonetheless, the CFD predictions agreed strongly with the experimental results for lactose powders SV003 and LH100.

The experimental validation results reported in this work suggest excellent promise for modelling entrainment of lactose powder drug formulations in DPIs with an EE CFD approach.

References

1. Labiris, N.R., Dolovich, M.B.: Pulmonary drug delivery. Part I: physiological factors affecting therapeutic effectiveness of aerosolized medications. *Brit. J. Clin. Pharm.* **56**(6), 588–599 (2003)
2. Kopsch, T., Murnane, D., Symons, D.: Optimizing the entrainment geometry of a dry powder inhaler: methodology and preliminary results. *Pharm. Res.* **33**(11), 2668–2679 (2016)
3. Parisini, I., Cheng, S.J., Symons, D., Murnane, D.: Potential of a cyclone prototype spacer to improve in vitro dry powder delivery. *Pharm. Res.* **31**(5), 1133–1145 (2014). <https://doi.org/10.1007/s11095-013-1236-8>
4. Zimarev, D., Parks, G., Symons, D.: Computational modelling and stochastic optimization of entrainment geometries in dry powder inhalers. In: DDL24 Conference (2013)
5. Ding, J., Gidaspow, D.: A bubbling fluidization model using kinetic theory of granular flow. *AIChE J.* **36**(4), 523–538 (1990). <https://doi.org/10.1002/aic.690360404>
6. The OpenFOAM Foundation. OpenFOAM 2.4. <http://www.openfoam.org/>
7. Gidaspow, D., Bezburaah, R., Ding, J.: Hydrodynamics of circulating fluidized beds: kinetic theory approach. In: Proceedings of the Seventh Engineering Foundation Conference on Fluidization (1992)
8. Johnson, P.C., Jackson, R.: Frictional-collisional constitutive relations for granular materials, with application to plane shearing. *J. Fluid Mech.* **176**(-1), 67 (1987). <https://doi.org/10.1017/S0022112087000570>
9. Lun, C.K.K., Savage, S.B., Jeffrey, D.J., Chepurmy, N.: Kinetic theories for granular flow: Inelastic particles in Couette flow and slightly inelastic particles in a general flowfield. *J. Fluid Mech.* **140**, 223–256 (1984). <https://doi.org/10.1017/S0022112084000586>
10. Sympatec GmbH. <http://www.sympatec.com/EN/LaserDiffraction/HELOS.html>. Accessed 15 June 2017 (2017)
11. Sympatec GmbH. <http://www.sympatec.com/EN/LaserDiffraction/RODOS.html>. Accessed 15 June 2017 (2017)
12. Copley Scientific. Quality Solutions for Inhaler Testing (2015)
13. TSI Inc. Certifier FA Ventilator test systems—for gas flow analysis (manual) (2010)

14. Casio Computer Co. Ltd. Digital Camera EX-FH20 User's guide (2008)
15. de Koning, J.P., van Der Mark, T.W., Coenegracht, P.M.J., Tromp, T.F.J., Frijlink, H.W.: Effect of an external resistance to airflow on the inspiratory flow curve. *Int. J. Pharm.* **234**(1–2), 257–266 (2002). [https://doi.org/10.1016/S0378-5173\(01\)00969-3](https://doi.org/10.1016/S0378-5173(01)00969-3)